TISSUE ENGINEERING: Part C
Volume 18, Number 1, 2012

DOI: 10.1089/ten.tec.2011.0216

Adipogenesis of Human Adipose-Derived Stem Cells Within Three-Dimensional Hollow Fiber-Based Bioreactors

Jörg C. Gerlach, M.D., Ph.D.,[1–3] Yen-Chih Lin, Ph.D.,[4] Candace A. Brayfield, Ph.D.,[1] Danielle M. Minteer, B.S.,[1] Han Li, M.D.,[4] J. Peter Rubin, M.D.,[1–4] and Kacey G. Marra, Ph.D.[1–4]

To further differentiate adipose-derived stem cells (ASCs) into mature adipocytes and create three-dimensional (3D) adipose tissue *in vitro*, we applied multicompartment hollow fiber-based bioreactor technology with decentral mass exchange for more physiological substrate gradients and integral oxygenation. We hypothesize that a dynamic 3D perfusion in such a bioreactor will result in longer-term culture of human adipocytes *in vitro*, thus providing metabolically active tissue serving as a diagnostic model for screening drugs to treat diabetes. ASCs were isolated from discarded human abdominal subcutaneous adipose tissue and then inoculated into dynamic 3D culture bioreactors to undergo adipogenic differentiation. Insulin-stimulated glucose uptake from the medium was assessed with and without TNF-alpha. 3D adipose tissue was generated in the 3D-bioreactors. Immunohistochemical staining indicated that 3D-bioreactor culture displayed multiple mature adipocyte markers with more unilocular morphologies as compared with two-dimensional (2D) cultures. Results of real-time polymerase chain reaction showed 3D-bioreactor treatment had more efficient differentiation in fatty acid-binding protein 4 expression. Repeated insulin stimulation resulted in increased glucose uptake, with a return to baseline between testing. Importantly, TNF-alpha inhibited glucose uptake, an indication of the metabolic activity of the tissue. 3D bioreactors allow more mature adipocyte differentiation of ASCs compared with traditional 2D culture and generate adipose tissue *in vitro* for up to 2 months. Reproducible metabolic activity of the adipose tissue in the bioreactor was demonstrated, which is potentially useful for drug discovery. We present here, to the best of our knowledge for the first time, the development of a coherent 3D high density fat-like tissue consisting of unilocular structure from primary adipose stem cells *in vitro*.

Introduction

As recently as 2010, nation-wide obesity rates continue to climb at an alarming rate. Circulating mononuclear cells from obesity causes inflammation, which, in turn, may cause diseased states such as diabetes.[1] You *et al.*[2] further demonstrated an increased pro-inflammatory cytokine production in obese humans, particularly in abdominal adipose tissue. Different approaches for controlling the obesity epidemic include expanding education programs about healthy living, reducing the marketing of unhealthy, high-fat foods, and providing low-cost exercise programs. Reducing obesity by increasing our understanding of adipose cell function and insulin resistance within adipose tissue is a potential strategy to help control the obesity epidemic.

Adult mesenchymal stem cells (MSCs) have the capacity for self-renewal and capability of differentiation to various cell lineages.[3] MSCs are found in various adult tissues, such as bone marrow, cartilage, and adipose tissue. Adipose tissue may be harvested from patients in a minimally invasive manner and provides a large quantity of autologous cells.[4] Adipose-derived stem cells (ASCs) derived from discarded human adipose tissue have many properties such as immunocompatibility and multipotency, rendering the cells ideal for regenerative medicine applications, such as cartilage, bone, soft tissue, and nerve repair.[5] Further, MSCs derived from adipose tissue possess the highest proliferation and differentiation potential, followed by MSCs derived from bone marrow and cartilage.[6] Differentiation into other phenotypes has also been reported. For example, Xu *et al.* demonstrated the differentiation of ASCs into Schwann cell-like cells. These cells may prove beneficial for the treatment of peripheral and central nerve injuries.[7] Kim *et al.* reported that human ASCs significantly improved motor recovery and enhanced morphometric change when implanted in contusive spinal cord injuries in rats.[8] de Mattos Carvalho

Departments of [1]Bioengineering and [2]Surgery, University of Pittsburgh, Pittsburgh, Pennsylvania.
[3]McGowan Institute for Regenerative Medicine, Pittsburgh, Pennsylvania.
[4]Division of Plastic and Reconstructive Surgery, University of Pittsburgh, Pittsburgh, Pennsylvania.

et al. evaluated the effect of ASCs in the treatment of induced tendinitis of the superficial digital flexor tendon in horses and observed increased perivascular inflammatory infiltrate, fibroblastic density, and qualitative healing improvement of tendon extracellular matrix.[9] Rabbit rear paw flexor tendons were acellularized and seeded with ASCs. After a bioreactor pretreatment, the ASCs contributed to the *in vitro* production of strong tendon material.[10] ASCs also can differentiate into osteocytes and chondrocytes.[11] Monaco *et al.*[12] reported that biomaterial scaffolds in combination with ASCs and growth factors provide a valuable tool for guided bone regeneration, especially for complex anatomic defects. Culturing of adipose precursor cells is typically performed in two-dimensional (2D) static culture by using Petri-dishes that provide a 2D culture surface.[13] The potent expansion of ASCs as well as comprehensive three-dimensional (3D) *in vitro* culture models of ASC differentiation will be of great significance in increasing the availability of ASCs for clinical use and to evaluate the efficacy of ASCs as a multifaceted tool. Moreover, the use of dynamic 3D perfusion bioreactors to expand and differentiate cells is currently being studied by several groups.[14–16] Bioreactor designs based on interwoven sets of semi-permeable hollow fibers in a multicompartment configuration compared with direct perfusion and rotating wall vessel suspension designs have the advantage of providing uniform nutrient and gas exchange with more physiological gradients and integral oxygenation, and—via the bicarbonate buffer system and CO_2 gas exchange—pH regulation to the entire cell compartment volume with negligible shear stresses. Such bioreactors offer a better environment for sustained long-term cultures of cell types not requiring mechanical stimuli. There have been many reports on the use of hollow fiber bioreactor designs used for hepatocyte cultures.[14,17–21] For example, Martin and Vermette have written a comprehensive review on the role of bioreactors for mass tissue culture.[14] Various types of bioreactors can be utilized, such as the hollow fiber-based bioreactors,[15–16] continuous stirred tank bioreactors,[22] rotating wall bioreactors,[23] Couette-Taylor bioreactors,[24] and shear flow perfusion bioreactors.[25]

There is a need for improved 3D systems to be used as high-throughput tools for drug discovery. Mature adipocyte cultures are particularly difficult within a traditional 2D plate culture due to their detachment from the surface on full differentiation and subsequent suspension within the media where they become extremely fragile. A 3D *in vitro* bioreactor system that allows long-term adipocyte culture with the ability to rapidly and effectively assay cytokine and adipokine expression, as well as test potential drug therapies, would be of great utility to endocrinologists, pharmacologists, and other researchers studying the associated mechanisms. We present an *in vitro* 3D perfusion model to study adipose tissue function, resulting in the long-term culture of metabolically active human adipose tissue.

Materials and Methods

Cell isolation

Adipose tissue (100–200 g) was harvested from the superficial abdominal depots of Caucasian women ($n=3$) undergoing elective abdominal reduction surgery. The patient age range was 40–60 years old, and all were healthy according to clinical examination and laboratory tests. The University of Pittsburgh Institutional Review Board approved the procedure of collecting the samples of adipose tissue. Samples were not pooled, with each experiment using cells from three different patients. Abdominal adipose tissue was placed in a 50 mL centrifuge tube (10 g per tube) and immersed in a 1 $mg \cdot mL^{-1}$ solution of collagenase. The isolated tissue was chopped with scissors and incubated at 37 °C for 35 min. The digested specimen was filtered and then centrifuged at 1000 rpm for 10 min. The pellet was suspended in erythrocyte lysis buffer. The solution was centrifuged again at 1000 rpm for 10 min. The pellet, which contained MSCs, was cultured in Dulbecco's modified Eagle's medium (DMEM)/F12 with 10% fetal bovine serum and 1% penicillin/streptomycin. Cells were passaged at confluency, and characterized as previously described by our laboratory.[26]

Bioreactor seeding

The bioreactor contains three independent hollow fiber membrane systems that are interwoven to repetitive subunits (Fig. 1). The extracapillary space forms a compartment in which up to 8×10^7 cultured cells are inoculated. The two independent medium fiber membrane systems are made of polyethersulfone capillary systems (Membrana) with a molecular-weight cutoff of MW 400,000. A hydrophobic multilaminate hollow fiber membrane system (Mitsubishi) enables gas supply. The total cell compartment inside the 3D hollow fiber-based bioreactor volume is 8 mL. The capillary network of the multicompartment bioreactor serves three functions: medium inflow, cell oxygenation/carbon dioxide removal, and medium outflow via countercurrent flow operation of the two medium membrane systems. As a result of interweaving a high performance mass exchange via countercurrent flow medium operation, decentralized gas supply and medium exchange with low gradients can be provided to the cultured cells. Bioreactor sterilization was performed with ethylene oxide gas at 60°C and degassed with air.

The initial experiments were performed by using pooled human deep abdominal and superficial abdominal preadipocytes for the bioreactor culture. Passage two cell suspensions were inoculated into the bioreactor and cultured throughout a period of 8 weeks. The cell compartments were continuously perfused with culture media via the PES hollow fiber bundles with a fresh feed rate of 4 $mL \cdot h^{-1}$ combined with a recirculation loop a the rate of 20 $mL \cdot min^{-1}$. Waste medium was removed from the circuit at 4 $mL \cdot h^{-1}$. The flows of compressed air and carbon dioxide in the gas compartment were maintained at 20 $mL \cdot min^{-1}$. Partial pressures of oxygen and carbon dioxide and acid/base status were regularly measured. The carbon dioxide content was adjusted to decreasing levels throughout culture time for maintaining the medium pH at 7.4.

Cell culture

For 3D adipogenic differentiation, after a 14-day expansion period by perfusion of plating media through the bioreactor cell compartment, the bioreactor feed media was subsequently changed for the next 3 weeks to subcutaneous differentiation medium (ZenBio). In parallel, 3×10^6 preadipocytes in the 2D control group were cultured with plating medium during the 14-day expansion period. Adipogenic differentiation was

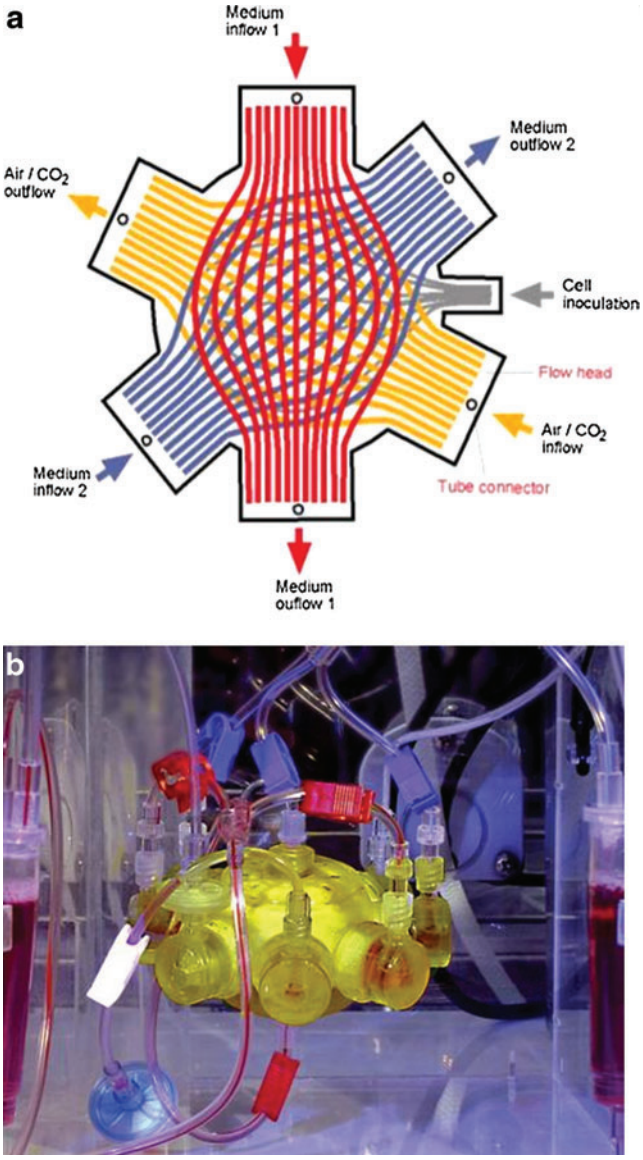

FIG. 1. **(a)** Diagram of laboratory scale 8 mL circuit hollow fiber-based bioreactor with perfusion system. **(b)** Photograph of laboratory scale hollow fiber-based bioreactor with perfusion system. Color images available online at www.liebertonline.com/tec

induced by using the defined adipogenic media just defined for the last 3 weeks.

Analysis of metabolic activity

Metabolic activity of the adipose tissue generated from expanded ASCs within the 3D hollow fiber-based bioreactors was assessed with glucose monitoring under an improved protocol with a dynamic open-circuit system. The two bioreactors seeded with the same patient cells that operated under the same conditions in parallel underwent three rounds of insulin stimulation with glucose measurements every 30 min for periods of 10–19 h. Feed inlet and waste outlet flow rate was set to 10 $mL \cdot h^{-1}$; therefore, the entire circuit volume was replaced every hour. The day before insulin stimulation, media was switched from low insulin-containing adipocyte maintenance medium to DMEM without insulin for the baseline glucose consumption of the tissue to stabilize at the set flow rate. For each round, glucose concentration measurements were taken a period of at least 2.5 h and up to 7 h to demonstrate a stable baseline glucose consumption of the tissue before adding insulin. Insulin stimulation was implemented by a step increase of the insulin concentration to 5 μM by a direct injection into the circuit and switching the feed media to insulin-containing DMEM to maintain a steady influx of insulin for a 4-h period. After the 4-h stimulation period, feed medium was switched back to noninsulin containing DMEM, and glucose concentration measurements were continued for 8 more hours to observe glucose consumption returning to baseline.

Histology

On culture day 60, the tissue/fiber samples were removed from the bioreactor for 10% buffered formalin fixed histology samples. Frozen bioreactor samples were stained with AdipoRed (AdipoRed Assay Reagent) to analyze lipid inclusion. Paraffin-embedded, formalin-fixed samples were stained with fatty acid-binding protein 4 (*FABP4*, a mature adipocyte marker; *FABP4* antibody, Millipore), glucose transporter 4 (GLUT 4; GLUT 4 antibody, Thermo Scientific), and peroxisome-proliferating activator receptor-γ (*PPAR-γ*, a mature adipocyte marker; Santa Cruz Biotechnology) to determine matrix formation and differentiation.

Gene expression and western blot analysis

RNA isolated at day 60 was used for quantitative polymerase chain reaction (qPCR). RNA was collected via Qiagen RNeasy mini Kit (Qiagen). Approximately 200 ng of total RNA was reverse-transcribed into cDNA by using First Strand Transcription Kit (Invitrogen), according to the manufacturer's protocol. The PCR primers were designed by using the Vector NTI (Invitrogen) and synthesized by Invitrogen. Efficiency was checked from tenfold serial dilutions of cDNA for each primer pair. A 2×SYBR® Green PCR Mastermix (Invitrogen), 0.1 μM of each primer, and the cDNA template were mixed in 25 μL volumes. qPCR was performed in triplicate in 96-well optical plates on Light Cycler 480 (Applied System). *β-Actin* was used as control for qPCR. All time points were compared relative to the unsorted cells in qPCR analyses.

Western blot analysis was measured by a modified protocol previously published by Choi *et al.*[27] For electrophoregram, 15 μL, 30 $\mu g \cdot mL^{-1}$ of the protein solution from each extract was added onto SDS polyacrylamide gel (Invitrogen NuPAGE gel), and electrophoretically transferred to a polyvinylidene difluoride (PVDF) membrane (Millipore). After blocking with PBS containing 5% skim milk (Nestle) and 0.1% Tween 20 (Sigma-Aldrich) for 2 h at room temperature, the membranes were incubated with monoclonal anti-*FABP4* from mouse (Santa Cruz Biotechnology), *β-actin* from mouse (Santa Cruz Biotechnology) as a standard for 1 h at room temperature. After washing thrice with TBS containing 1% skim milk and 0.1% Tween 20, the membranes were incubated with anti-mouse IgG, Rabbit HRP antibody (Jackson ImmunoResearch) for 1 h at room temperature. The membranes were washed three more times, and the signals were visualized via a reaction with an enhanced chemiluminescence (ECL) plus

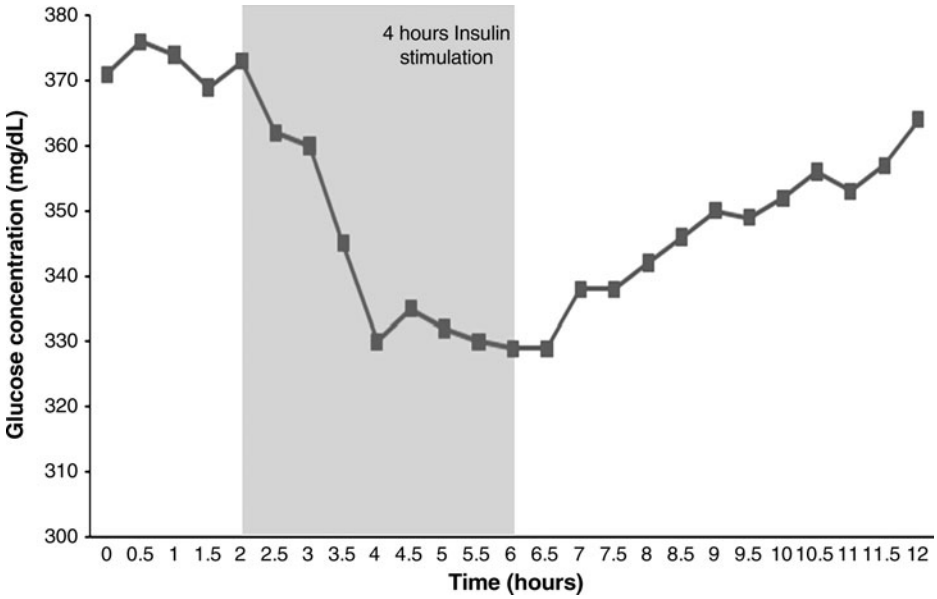

FIG. 2. Two three-dimensional (3D) hollow fiber-based bioreactors were operated simultaneously with cells from the same patient: 4 h insulin stimulation period with glucose consumption ($n = 6$).

western blotting detection regent (GE Healthcare) for 15 min. Image analyses were performed with a Molecular Imager Chemi Doc XRS image system (BioRad).

Statistics

All results will be presented as mean ± standard deviation. Unpaired *t*-tests were performed to assess differences in treatment groups. Statistical significance will be set at a *p*-value less than or equal to 0.05.

Results

Analysis of metabolic activity

Figure 2 represents a plot of the glucose concentrations before, during, and after insulin stimulation of adipose tissue Change to Bllded put from ASCs within the one 3D hollow fiber-based bioreactors. The result indicate stable baseline glucose consumption of the tissue over a 4-h period, with insulin stimulation occurring from the second hour. The glucose concentration dropped substantially over the 4-h period to give a change in glucose concentration of 370 $mg \cdot dL^{-1}$ for one bioreactor and 330 $mg \cdot dL^{-1}$ in the other. Figure 3 represents the overall glucose consumption induced during the insulin stimulation period whereby the glucose concentration at the end of the 4-h stimulation period is subtracted from the glucose concentration at the beginning of the 4-h stimulation period. 3D hollow fiber-based bioreactors were pretreated with tumor necrosis factor (TNF)-α 24 h before the insulin was added. The standard deviation on the first "bioreactor" bar is for three separate rounds of insulin stimulation, to show the reproducibility within one bioreactor. This is significant, because it shows that we could potentially test a drug five times on the same tissue. Results indicate that TNF-α treatment inhibited the cells from consuming as much glucose compared with trials without TNF-α.

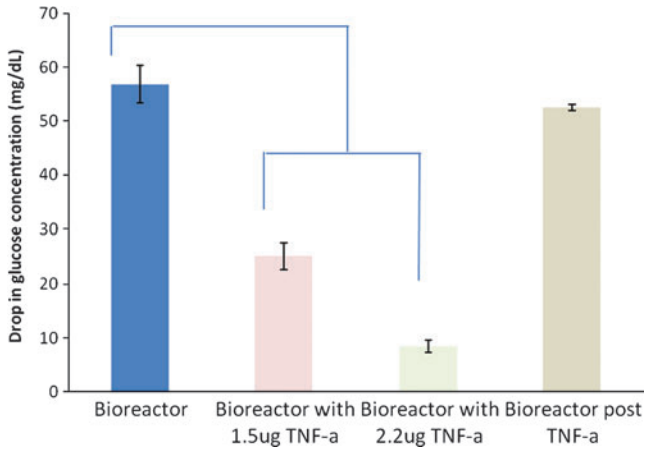

FIG. 3. Two 3D hollow fiber-based bioreactors were operated simultaneously with cells from the same patient: 24 h pretreatment of TNF-α stimulation and 4 h insulin stimulation period with glucose consumption ($n = 6$). TNF-α, tumor necrosis factor-α. Color images available online at www.liebertonline.com/tec

Histological staining

Tissue morphology results of the tissue generated within the 3D hollow fiber-based bioreactors are displayed in Figures 4 and 5. Dense macroscopic tissue formation was observed in and around hollow fiber membranes by the end of each differentiation period. Confocal microscope imaging of the bioreactor tissue intact as whole tissue revealed closely associated adipocytes throughout, resembling natural adipose tissue. Confocal fluorescent imagining demonstrated significant *FABP4*, GLUT 4, and *PPAR-γ* staining within most cells contained within the bioreactor tissue. AdipoRed staining revealed cells to have more unilocular lipid-filled vacuoles compared with multilocular lipid droplets of ASCs differentiated in 2D cultures.

Gene and protein expression

The results of real-time PCR demonstrate that the 3D-bioreactor treatment had a more efficient differentiation in

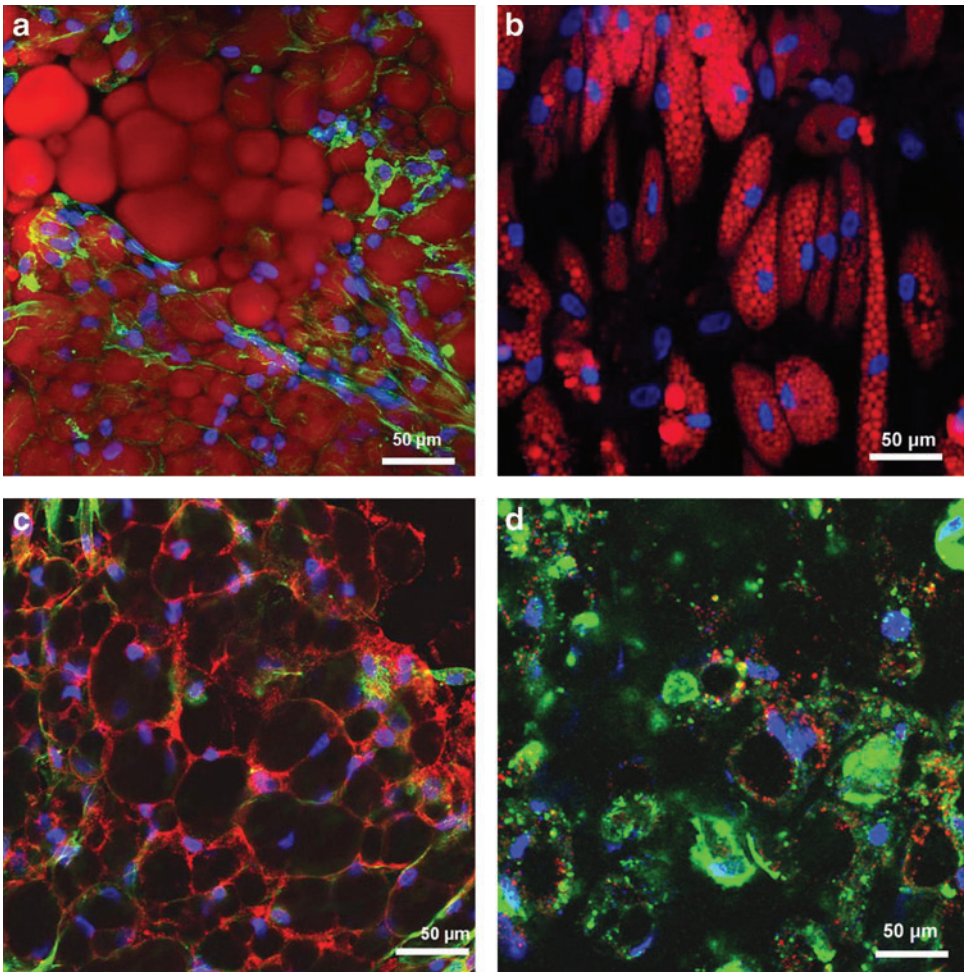

FIG. 4. Confocal microscopy reconstructed stacks of 3D adipose tissue generated within the bioreactors **(a, c)** and two-dimensional (2D) control treatment **(b, d)**. All samples stained with DAPI (blue), Phalloidin-AlexaFluor 488 (green), and the following fluorescent markers using Cy3 (red): **(a, b)** AdipoRed (demonstrating lipid accumulations) markers, and **(c, d)** Glucose transporter 4 (GLUT 4). Single image *z*-stack reconstructions throughout a 50-µm depth of the 3D samples ($n=6$). DAPI, 4′, 6-diamino-2-phenylindole. Color images available online at www.liebertonline.com/tec

FABP4 and *PPAR-γ* expression (Fig. 6a). Western blot compares *FABP4* protein (a mature adipocyte marker), expression detection from ASCs cultured in bioreactor, 2D culture flask, and natural fat tissue (Fig. 6b). Western blot results suggest no significant difference of *FABP4* protein expression between 3D hollow fiber-based bioreactor treatment and native fat tissue.

Discussion

Adipose tissue plays not only an important role in obesity, but is also increasingly acknowledged as a potent endocrine organ involved in many physiological processes. Elucidation of molecular and cellular adipocyte differentiation and metabolism processes will lead to prevention and treatment of obesity and resulting complications.[28] However, only limited references exist regarding cell-cell or cell-extracellular matrix interactions within adipose tissue in 3D adipogenic culture.[29] We present here, to the best of our knowledge for the first time, the development of a coherent 3D high density fat-like tissue consisting of unilocular structure from primary adipose stem cells *in vitro*.

During the differentiation period with circulating adipogenic media, glucose consumption and lactate production steadily increased, possibly due to differentiating cells storing glucose for lipid accumulation similar to adipocyte function. Glycerol production rapidly increased initially, decreased for 14 days, and then maintained a steady increase throughout the differentiation period. In an *in vivo* situation, adipocytes within whole adipose tissue secrete a low level of glycerol free fatty acids, and are termed the "basal lipolysis" of the cells.[30–32] An increase in obesity among patients results in a subsequent increase in basal lipolysis levels from expanding adipose tissue.[31] Therefore, the glycerol production assay performed on the bioreactor recirculation media samples was used to indirectly monitor an increased differentiation of the cultured cells due to the addition of adipogenic media. The increase in basal lipolysis levels observed *in vivo* with increasing adipose tissue mass is also observed in the bioreactor culture with an increase in adipogenic differentiation during the last 3 weeks. The adipogenic differentiation of the preadipocyte cells was further confirmed with imaging of the tissue. As described in Figure 2, the architecture of the cells cultured in the 3D bioreactor better resembles the architecture of natural adipose tissue than do the cells grown in traditional 2D culture. Metabolic activity of the adipose tissue within the 3D hollow fiber-based bioreactor was assessed with glucose monitoring with and without insulin stimulation at the end of the culture period before shut down of the bioreactor system. The protocol used to measure glucose consumption by the tissue during such tests was

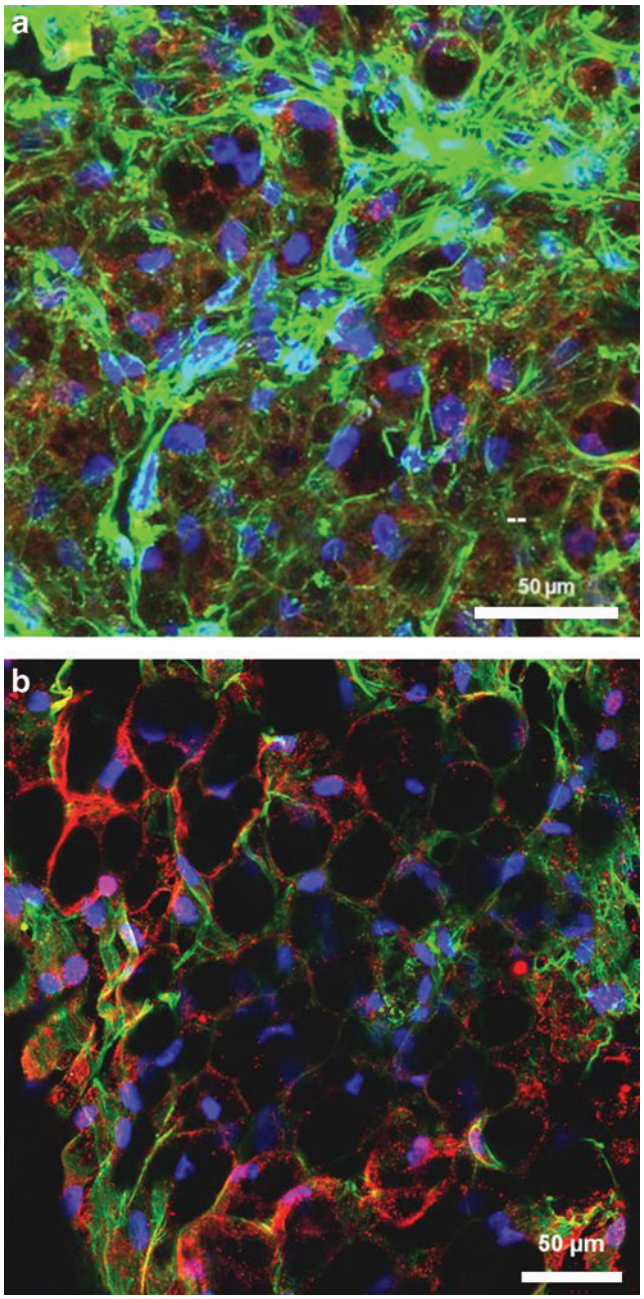

FIG. 5. Confocal microscopy reconstructed stacks of 3D adipose tissue generated within the bioreactors. All samples stained with DAPI (blue) and Phalloidin-AlexaFluor 488 (green), and the following fluorescent markers using Cy3 (red): **(a)** Fatty acid binding-protein 4 (*FABP4*, a mature adipocyte marker) markers, and **(b)** Peroxisome-proliferating activator receptor-γ (*PPAR-γ*, a mature adipocyte marker). Single image *z*-stack reconstructions throughout a 50-μm depth of the 3D samples ($n=6$). Color images available online at www.liebertonline.com/tec

performed with the tubing circuit closed starting with a finite amount of glucose in the media. Five separate rounds of insulin stimulation were performed on the same bioreactor tissue with baseline (without insulin) measurements taken first and the circuit then refilled with medium and two insulin doses added at 0 and 240 min (bringing the insulin concentration within the closed circuit to 2 μM with the first dose). Glucose concentration measurements were taken every 30 min over a 360 min period within each round (all data in Fig. 2). Rounds were performed every other day, with the third round pretreated for 24 h with 10 $ng \cdot mL^{-1}$ TNF-α to inhibit insulin stimulated glucose uptake during the third round of measurements. The fourth and fifth rounds were performed at 2 and 5 days, respectively, after the third measurement round to observe reversibility of TNF-α inhibition. The first two rounds of measurements demonstrated substantially higher insulin-stimulated glucose uptake by the bioreactor tissue than the baseline glucose consumption without insulin. The third round of measurements demonstrated TNF-α induced inhibition lowering glucose consumption of both baseline and insulin stimulated periods compared with the first two rounds. The fifth round of testing indicated a reversible effect on baseline glucose consumption after TNF-α treatment after a period of only 5 days, whereas the insulin-stimulated glucose consumption had not yet returned to normal.

Stem cells are defined by the ability to either self-renew or differentiate into multiple cell lineages.[33]MSCs are often targeted for tissue engineering due to their vital role in native tissue formation and function.[34] The first aim of our study was to investigate that 3D primary adipose stem cells culture leads to completion of adipose tissue formation *in vitro* in a long-term period. Histological staining results illustrate that culturing 3D, adipose-like tissue is feasible in all batches of hollow fiber-based bioreactor. AdipoRed staining reveals lipid-loading indicative of mature adipose tissue (Fig. 4). The generated tissue is composed of living cells at varying stages of maturity. Moreover, cells remain viable in the interior of aggregate as opposed to forming necrotic cores, as reported with other tissues grown in bioreactor systems.[28] A few studies report the use of 3D bioreactors for adipose-derived stem cell or also preadipocyte culture. One study by Fischbach *et al.* utilized biodegradable poly(glycolic acid) fiber meshes seeded with the murine preadipocyte cell line, 3T3-L1.[29] The constructs were dynamically cultured in a spinner flask for up to 2 weeks. The murine preadipocytes were differentiated into mature adipocytes, with adipogenesis occurring more rapidly in the dynamic seeding device as compared with a static culture. In another report, Patrick *et al.* described the potential of adipose tissue formation by using a 3D bioreactor culture system.[35] Although no experimental details were provided, an image of 3D adipose tissue created from the bioreactor culture was shown. In our results, tissue was obtained from a hollow fiber-based bioreactor cell compartment at the end of the culture period. Tissue is generated between hollow fibers used for media and gas perfusion, and the morphology appeared similar to adipose-like tissue. *FABP4* and *PPAR-γ* mRNA gene expression is shown in Figure 6. These results likely reflect the uneven distribution of adipose tissue throughout the bioreactor. Further study involves examining the distribution of new tissue in the bioreactor during long-term culture.

Overall, we have demonstrated the utilization of a multi-compartment 3D perfusion bioreactor technology to facilitate the long-term culture of adipose tissue *in vitro*.

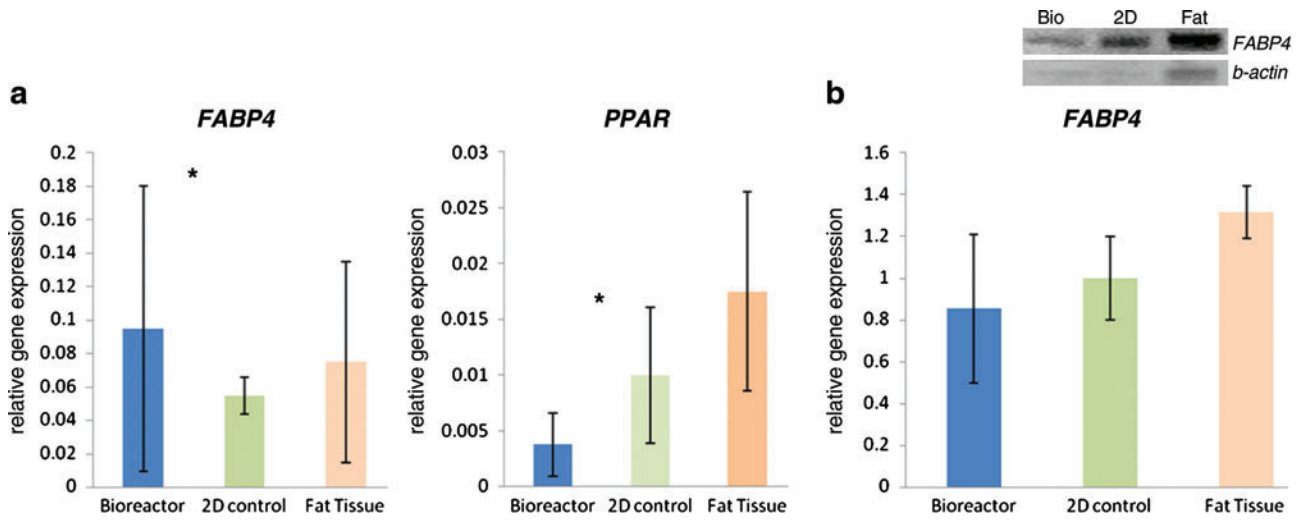

FIG. 6. **(a)** Quantitative RT-PCR results comparing gene expression ratios for *FABP4* (a mature adipocyte marker), and *PPAR-γ* (a mature adipocyte marker) gene expression detection from adipose-derived stem cells (ASCs) cultured in the bioreactor, 2D flask, and nature fat tissue. **(b)** Western blot comparing *FABP4* protein (a mature adipocyte marker) expression detection from ASCs cultured in bioreactor, 2D flask, and nature fat tissue. Western blot of *FABP4* and *β-actin* protein expression. The control group is 2D cultured treatment. *Significantly different between groups, $p < 0.05$ ($n = 10$). RT-PCR, reverse transcription polymerase chain reaction. Color images available online at www.liebertonline.com/tec

Conclusion

We envision that expansion and differentiation of ASCs in a 3D perfusion bioreactor will provide useful technology toward a further understanding of adipogenesis *in vitro* models, and we anticipate sharing the model with other researchers. Our technology should assist in discovering new treatments for obesity and diabetes, as well as other metabolic disorders.

Acknowledgments

The work presented has been supported by the National Institute of Health (1R01DK089190-01) (KGM) and Pfizer, Inc. (J.P.R.). The authors would like to acknowledge the Center for Biologic Imaging (University of Pittsburgh) for assistance with imaging; M. Thiede, K. Haskell, N. Oyster and M. Young for technical assistance.

Disclosure statement

The authors state that no competing financial interests exist.

References

1. Ghanim, H., Aljada, A., Hofmeyer, D., Syed, T., Mohanty, P., and Dandona, P. Circulating mononuclear cells in the obese are in a proinflammatory state. Circulation **110,** 1564, 2004.
2. You, T., Yang, R., Lyles, M.F., Gong, D., and Nicklas, B.J. Abdominal adipose tissue cytokine gene expression: relationship to obesity and metabolic risk factors. Am J Physiol Endocrinol Metab **288,** 741, 2005.
3. Bajada, S., Mazakova, I., Richardson, J.B., and Ashammakhi, N. Updates on stem cells and their applications in regenerative medicine. J Tissue Eng Regen Med **20,** 169, 2008.
4. Wei, Y., Wei, Y.H., Han, H.Y., Meng, G., Zhang, D., Wu, Z., *et al.* A novel injectable scaffold for cartilage tissue engineering using adipose-derived adult stem cells. J Orthop Res **26,** 27, 2008.
5. Santiago, L.Y., Nowak, R.W., Peter Rubin, J., and Marra, K.G. Peptide-surface modification of poly(caprolactone) with laminin-derived sequences for adipose-derived stem cell applications. Biomaterials **27,** 2962, 2006.
6. Peng, L., Jia, Z., Yin, X., Zhang, X., Liu, Y., Chen, P., *et al.* Comparative analysis of mesenchymal stem cells from bone marrow, cartilage and adipose tissue. Stem Cells Dev **17,** 761, 2008.
7. Xu, Y., Liu, L., Li, Y., Zhou, C., Xiong, F., Liu, Z., *et al.* Myelin-forming ability of Schwann cell-like cells induced from rat adipose-derived stem cells *in vitro.* Brain Res **1239,** 49, 2008.
8. Kim, S.B., and Kwak, H. Poster 278: the effects of human adipose tissue-derived mesenchymal stem cells transplantation on neurologic recovery in rats with spinal cord injury. Arch Phys Med Rehabil **88,** E91, 2007.
9. de Mattos Carvalho, A., Alves, A.L.G., de Oliveira, P.G.G., Cisneros Alvarez, L.E., Amorim, R.L., Hussni, C.A., *et al.* Use of adipose tissue-derived mesenchymal stem cells for experimental tendinitis therapy in equines. J Equine Vet Sci **31,** 26, 2011.
10. Angelidis, I.K., Thorfinn, J., Connolly, I.D., Lindsey, D., Pham, H.M., and Chang, J. Tissue engineering of flexor tendons: the effect of a tissue bioreactor on adipoderived stem cell-seeded and fibroblast-seeded tendon constructs. J Hand Surg **35,** 1466, 2010.
11. Krampera, M., Pizzolo, G., Aprili, G., and Franchini, M. Mesenchymal stem cells for bone, cartilage, tendon and skeletal muscle repair. Bone **39,** 678, 2006.
12. Monaco, E., Bionaz, M., Hollister, S.J., and Wheeler, M.B. Strategies for regeneration of the bone using porcine adult adipose-derived mesenchymal stem cells. Theriogenology **75,** 1381, 2011.
13. Kirkland, J.L., Hollenberg, C.H., and Gillon, W.S. Age, anatomic site, and the replication and differentiation of adipocyte precursors. Am J Physiol **258,** C206, 1990.
14. Martin, Y., and Vermette, P. Bioreactors for tissue mass culture: design, characterization, and recent advances. Biomaterials **26,** 7481, 2005.

15. Ho Ye, S., Watanabe, J., Takai, M., Iwasaki, Y., and Ishihara, K. High functional hollow fiber membrane modified with phospholipid polymers for a liver assist bioreactor. Biomaterials **27,** 1955, 2006.
16. Monga, S., Hout, M., Baun, M., Micsenyi, A., Muller, P., Tummalapalli, L., *et al.* Mouse fetal liver cells in artificial capillary beds in three-dimensional four-compartment bioreactors. Am J Pathol **167,** 1279, 2005.
17. Potter, K., Butler, J., Adams, C., Fishbein, K., McFarland, E., and Horton, W. Cartilage formation in a hollow fiber bioreactor studied by proton magnetic resonance microscopy. Matrix Biol **17,** 513, 1998.
18. Sussman, N., and Kelly, J. Improved liver function following treatment with an extracorporeal liver assist device. Artif Organs **17,** 27, 1993.
19. Watanabe, F., Mullon, C., Hewitt, W., Arkadopoulos, N., Kahaku, E., Eguchi, S., *et al.* Clinical experience with a bioartificial liver in the treatment of severe liver failure. A phase I clincial trial. Ann Surg **225,** 484, 1997.
20. Meng, Q., Zhang, G., and Wu, D. Hepatocyte culture in bioartificial livers with different membrane characteristics. Biotechnol Lett **26,** 1407, 2004.
21. Dixit, V. Development of a bioartifical liver using isolated hepatocytes. Artif Organs **18,** 371, 1994.
22. Chen, C., Chen, K., and Yang, S. Effects of three-dimensional culturing on osteosarcoma cells grown in a fibrous matrix: analyses of cell morphology, cell cycle, and apoptosis. Biotechnol Prog **19,** 1574, 2003.
23. Lin, H., O'Shaughnessy, T., Kelly, J., and Ma, W. Neural stem cell differentiation in a cell-collagen-bioreactor culture system. Brain Res Dev Brain Res **153,** 163, 2004.
24. Haut, B., Ben Amor, H., Coulon, L., Jacquet, A., and Halloin, V. Hydrodynamics and mass transfer in a Couette-Taylor bioreactor for the culture of animal cells. Chem Eng Sci **58,** 777, 2003.
25. Gomes, M., Bossano, C., Johnston, C., Reis, R., and Mikos, A. *In vitro* localization of bone growth factors in constructs of biodegradable scaffolds seeded with marrow stromal cells and cultured in a flow perfusion bioreactor. Tissue Eng **12,** 177, 2006.
26. Lin, Y.-C., Brayfield, C.A., Gerlach, J.C., Peter Rubin, J., and Marra, K.G. Peptide modification of polyethersulfone surfaces to improve adipose-derived stem cell adhesion. Acta Biomaterialia **5,** 1416, 2009.
27. Choi, Y.S., Parka, S.-N., and Suh, H. Adipose tissue engineering using mesenchymal stem cells attached to injectable PLGA spheres. Biomaterials **26,** 5855, 2005.
28. Frye, C.A., and Patrick, C.W. Three-dimensional adipose tissue model using low shear bioreactors. In Vitro Cell Dev Biol **42,** 109, 2006.
29. Fischbach, C., Seufert, J., Staiger, H., Hacker, M., Neubauer, M., Gopferich, A., *et al.* Three-dimensional *in vitro* model of adipogenesis: comparison of culture conditions. Tissue Eng **10,** 215, 2004.
30. Ramis, J.M., Salinas, R., Garcia-Sanz, J.M., Moreiro, J., Proenza, A.M., and Llado, I. Depot- and gender-related differences in the lipolytic pathway of adipose tissue from severely obese patients. Cell Phys Biochem **17,** 173, 2006.
31. Lofgren, P., Hoffstedt, J., Ryden, M., Thorne, A., Holm, C., and Wahrenberg, H., *et al.* Major gender differences in the lipolytic capacity of abdominal subcutaneous fat cells in obesity observed before and after long-term weight reduction. J Clin Endocr Metab **87,** 764, 2002.
32. Kissebah, A., Vydelingum, N., Murray, R., Evans, D., Hartz, A., Kalkhoff, R., *et al.* Relation of body fat distribution to metabolic complications of obesity. J Clin Endocrinol Metab **54,** 254, 1982.
33. King, J.A., and Miller, W.M. Bioreactor development for stem cell expansion and controlled differentiation. Curr Opin Chem Biol **11,** 394, 2007.
34. Liao, J., Guo, X., Grande-Allen, K.J., Kasper, F.K., and Mikos, A.G. Bioactive polymer/extracellular matrix scaffolds fabricated with a flow perfusion bioreactor for cartilage tissue engineering. Biomaterials **31,** 8911, 2010.
35. Patrick, C.W., Jr. Breast tissue engineering. Annu Rev Biomed Eng **6,** 109, 2004.

Address correspondence to:
Kacey G. Marra, Ph.D.
Department of Surgery
1655E Biomedical Science Tower
200 Lothrop St.
University of Pittsburgh
Pittsburgh, PA 15261

E-mail: marrak@upmc.edu

Received: April 14, 2011
Accepted: September 1, 2011
Online Publication Date: October 13, 2011